

Signal Propagation in Feedforward Neuronal Networks with Unreliable Synapses

Daqing Guo^{1*}, Chunguang Li^{2†}

¹ School of Electronic Engineering, University of Electronic Science and Technology of China, Chengdu 610054, People's Republic of China

² Department of Information Science and Electronic Engineering, Zhejiang University, Hangzhou 310027, People's Republic of China

November 6, 2018

Abstract

In this paper, we systematically investigate both the synfire propagation and firing rate propagation in feedforward neuronal network coupled in an all-to-all fashion. In contrast to most earlier work, where only reliable synaptic connections are considered, we mainly examine the effects of unreliable synapses on both types of neural activity propagation in this work. We first study networks composed of purely excitatory neurons. Our results show that both the successful transmission probability and excitatory synaptic strength largely influence the propagation of these two types of neural activities, and better tuning of these synaptic parameters makes the considered network support stable signal propagation. It is also found that noise has significant but different impacts on these two types of propagation. The additive Gaussian white noise has the tendency to reduce the precision of the synfire activity, whereas noise with appropriate intensity can enhance the performance of firing rate propagation. Further simulations indicate that the propagation dynamics of the considered neuronal network is not simply determined by the average amount of received neurotransmitter for each neuron in a time instant, but also largely influenced by the stochastic effect of neurotransmitter release. Second, we compare our results with those obtained in corresponding feedforward neuronal networks connected with reliable synapses but in a random coupling fashion. We confirm that some differences can be observed in these two different feedforward neuronal network models. Finally, we study the signal propagation in feedforward neuronal networks consisting of both excitatory and inhibitory neurons, and demonstrate that inhibition also plays an important role in signal propagation in the considered networks.

*Email: dqguo07@gmail.com

†Author for correspondence, Email: cgli@zju.edu.cn

Keywords: Feedforward neuronal network, unreliable synapse, signal propagation, synfire chain, firing rate

1 Introduction

A major challenge in neuroscience is to understand how the neural activities are propagated through different brain regions, since many cognitive tasks are believed to involve this process (Vogels and Abbott, 2005). The feedforward neuronal network is the most used model in investigating this issue, because it is simple enough yet can explain propagation activities observed in experiments. In recent years, two different modes of neural activity propagation have been intensively studied. It has been found that both the synchronous spike packet (*synfire*), and the *firing rate*, can be transmitted across deeply layered networks (Abeles 1991; Aertsen et al. 1996; Diesmann et al. 1999; Diesmann et al. 2001; Câteau and Fukai 2001; Gewaltig et al. 2001; Tetzlaff et al. 2002; Tetzlaff et al. 2003; van Rossum et al. 2002; Vogels and Abbott 2005; Wang et al. 2006; Aviel et al. 2003; Kumar et al. 2008; Kumar et al. 2010; Shinozaki et al. 2007; Shinozaki et al. 2010). Although these two propagation modes are quite different, the previous results demonstrated that a single network with different system parameters can support stable and robust signal propagation in both of the two modes, for example, they can be bridged by the background noise and synaptic strength (van Rossum et al. 2002; Masuda and Aihara 2002; Masuda and Aihara 2003).

Neurons and synapses are fundamental components of the brain. By sensing outside signals, neurons continually fire discrete electrical signals known as action potentials or so-called spikes, and then transmit them to postsynaptic neurons through synapses (Dayan and Abbott 2001). The spike generating mechanism of cortical neurons is generally highly reliable. However, many studies have shown that the communication between neurons is, by contrast, more or less unreliable (Abeles 1991; Raastad et al. 1992; Smetters and Zador 1996). Theoretically, the synaptic unreliability can be explained by the phenomenon of probabilistic transmitter release (Branco and Staras 2009; Katz 1966; Katz 1969; Trommershäuser et al. 1999), i.e., synapses release neurotransmitter in a stochastic fashion, which has been confirmed by well-designed biological experiments (Allen and Stevens 1994). In most cases, the transmission failure rate at a given synapse tends to exceed the fraction of successful transmission (Rosenmund et al. 1993; Stevens and Wang 1995). In some special cases, the synaptic transmission failure rate can be as high as 0.9 or even higher (Allen and Stevens 1994). Further computational studies have revealed that the unreliability of synaptic transmission might be a part of information processing of the brain and possibly has functional roles in neural computation. For instance, it has been reported that the unreliable synapses provide a useful mechanism for reliable analog computation in space-rate coding (Maass and Natschläger 2000); and it has been found that suitable synaptic successful transmission probability can improve the information transmission efficiency of synapses (Goldman 2004) and can filter the redundancy information by removing autocorrelations in spike trains (Goldman et al. 2002). Furthermore, it has also been demonstrated that unreliable synapses largely influence both the emergence and dynamical behaviors of clusters in an all-to-all pulse-coupled neuronal network, and can make the whole network relax to clusters of identical size (Friedrich and Kinzel 2009).

Although the signal propagation in multilayered feedforward neuronal networks has been extensively studied, to the best of our knowledge the effects of unreliable synapses on the propagation of neural activity have not been widely discussed and the relevant questions still remain unclear (but see the footnote¹). In this paper, we address these questions and provide insights by computational modeling. For this purpose, we examine both the synfire propagation and firing rate propagation in feedforward neuronal networks. We mainly investigate the signal propagation in feedforward neuronal networks composed of purely excitatory neurons connected with unreliable synapses in an all-to-all coupling fashion (abbr. URE feedforward neuronal network) in this work. We also compare our results with the corresponding feedforward neuronal networks (we will clarify the meaning of “corresponding” later) composed of purely excitatory neurons connected with reliable synapses in a random coupling fashion (abbr. RRE feedforward neuronal network). Moreover, we study feedforward neuronal networks consisting of both excitatory and inhibitory neurons connected with unreliable synapses in an all-to-all coupling fashion (abbr. UREI feedforward neuronal network).

The rest of this paper is organized as follows. The network architecture, neuron model, and synapse model used in this paper are described in Sec. 2. Besides these, the measures to evaluate the performance of synfire propagation and firing rate propagation, as well as the numerical simulation method are also introduced in this section. The main results of the present work are presented in Sec. 3. Finally, a detailed conclusion and discussion of our work are given in Sec. 4.

2 Model and method

2.1 Network architecture

In this subsection, we introduce the network topology used in this paper. Here we only describe how to construct the URE feedforward neuronal network. The methods about how to build the corresponding RRE feedforward neuronal network and the UREI feedforward neuronal network will be briefly given in Secs. 3.4 and 3.5, respectively. The architecture of the URE feedforward neuronal network is schematically shown in Figure 1. The network totally contains $L = 10$ layers, and each layer is composed of $N_s = 100$ excitatory neurons. Since neurons in the first layer are responsible for receiving and encoding the external input signal, we therefore call this layer sensory layer and neurons in this layer are called sensory neurons. In contrast, the function of neurons in the other layers is to propagate neural activities. Based on this reason, we call these layers transmission layers and the corresponding neurons cortical neurons. Because the considered neuronal network is purely feedforward, there is no feedback connection from neurons in downstream layers to neurons in upstream layers, and there is also no connection among neurons within the same layer. For simplicity, we call the i -th neuron in the

¹An anonymous reviewer kindly reminded us that there might be a relevant abstract (Trommershäuser and Diesmann 2001) discussing the effect of synaptic variability on the synchronization dynamics in feedforward cortical neural networks, but the abstract itself does not contain the results presumably presented on the poster and also the follow-up publications do not exist.

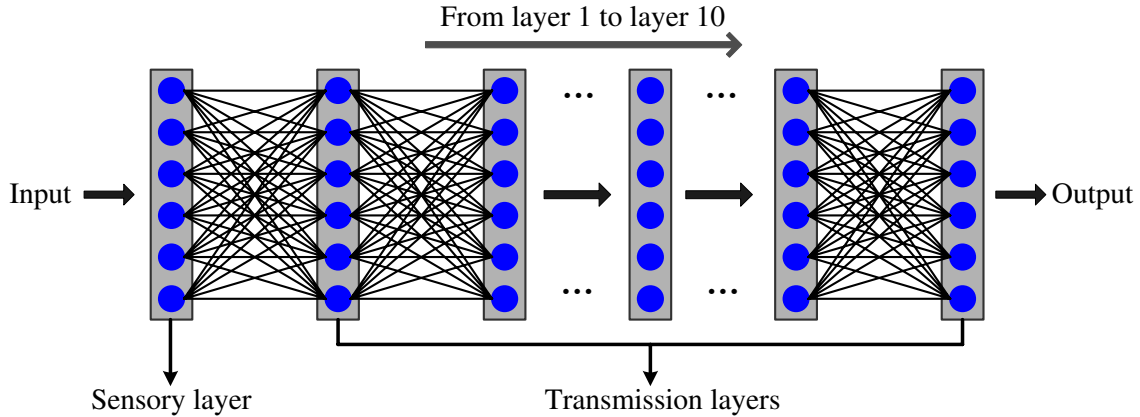


Figure 1: Network architecture of the URE feedforward neuronal network. The network totally contains 10 layers. The first layer is the sensory layer and the others are the transmission layers. Each layer consists of 100 excitatory neurons. For clarity, only 6 neurons are shown in each layer.

j -th layer neuron (i, j) in the following.

2.2 Neuron model

We now introduce the neuron model used in the present work. Each cortical neuron is modeled by using the integrate-and-fire (IF) model (Nordlie et al. 2009), which is a minimal spiking neuron model to mimic the action potential firing dynamics of biological neurons. The subthreshold dynamics of a single IF neuron obeys the following differential equation:

$$\tau_m \frac{dV_{ij}}{dt} = V_{\text{rest}} - V_{ij} + RI_{ij}, \quad (2.1)$$

with the total input current

$$I_{ij} = I_{ij}^{\text{syn}} + I_{ij}^{\text{noise}}. \quad (2.2)$$

Here $i = 1, 2, \dots, N_s$ and $j = 2, 3, \dots, L$, V_{ij} represents the membrane potential of neuron (i, j) , $\tau_m = 20$ ms is the membrane time constant, $V_{\text{rest}} = -60$ mV is the resting membrane potential, $R = 20$ M Ω denotes the membrane resistance, and I_{ij}^{syn} is the total synaptic current. The noise current $I_{ij}^{\text{noise}} = \sqrt{2D_t}\xi_{ij}(t)$ represents the external or intrinsic fluctuations of the neuron, where $\xi_{ij}(t)$ is a Gaussian white noise with zero mean and unit variance, and D_t is referred to as the noise intensity of the cortical neurons. In this work, a deterministic threshold-reset mechanism is implemented for spike generation. Whenever the membrane potential of a neuron reaches a fixed threshold at $V_{\text{th}} = -50$ mV, the neuron fires a spike, and then the membrane potential is reset according to the resting potential, where it remains clamped for a 5-ms refractory period.

On the other hand, we use different models to simulate the sensory neurons depending on different tasks. To study the synfire propagation, we assume that each sensory neuron is a simple spike generator, and control their firing behaviors by ourselves. While studying the firing rate propagation, the sensory neuron is modeled by using the IF neuron model with the same expression (see Eq. (2.1)) and the same parameter settings as those for cortical neurons. For each sensory neuron, the total input current is given by

$$I_{i1} = I(t) + I_{i1}^{\text{noise}}, \quad (2.3)$$

where $i = 1, 2, \dots, N_s$ index neurons. The noise current I_{i1}^{noise} has the same form as that for cortical neurons but with the noise intensity D_s . $I(t)$ is a time-varying external input current which is injected to all sensory neurons. For each run of the simulation, the external input current is constructed by the following process. Let $\eta(t)$ denote an Ornstein-Uhlenbeck process, which is described by

$$\tau_c \frac{d\eta(t)}{dt} = -\eta(t) + \sqrt{2A}\xi(t), \quad (2.4)$$

where $\xi(t)$ is a Gaussian white noise with zero mean and unit variance, τ_c is a correlation time constant, and A is a diffusion coefficient. The external input current $I(t)$ is defined as

$$I(t) = \begin{cases} \eta(t) & \text{if } \eta(t) \geq 0, \\ 0 & \text{if } \eta(t) < 0. \end{cases} \quad (2.5)$$

Parameter A can be used to denote the intensity of the external input signal $I(t)$. In this work, we choose $A = 200 \text{ nA}^2$ and $\tau_c = 80 \text{ ms}$. By its definition, the external input current $I(t)$ corresponds to a Gaussian-distributed white noise low-pass filtered at 80 ms and half-wave rectified. It should be noted that this type of external input current is widely used in the literature, in particular in the research papers which study the firing rate propagation (van Rossum et al. 2002; Vogels and Abbott 2005; Wang and Zhou 2009).

2.3 Synapse model

The synaptic interactions between neurons are implemented by using the modified conductance-based model. Our modeling methodology is inspired by the phenomenon of probabilistic transmitter release of the real biological synapses. Here we only introduce the model of unreliable excitatory synapses, because the propagation of neural activity is mainly examined in URE feedforward neuronal networks in this work. The methods about how to model reliable excitatory synapses and unreliable inhibitory synapses will be briefly introduced in Secs. 3.4 and 3.5, respectively.

The total synaptic current onto neuron (i, j) is the linear sum of the currents from all incoming synapses,

$$I_{ij}^{\text{syn}} = \sum_{k=1}^{N_s} G(i, j; k, j-1) \cdot (E_{\text{syn}} - V_{ij}). \quad (2.6)$$

In this equation, the outer sum runs over all synapses onto this particular neuron, $G(i, j; k, j - 1)$ is the conductance from neuron $(k, j - 1)$ to neuron (i, j) , and $E_{\text{syn}} = 0$ mV is the reversal potential of the excitatory synapse. Whenever the neuron $(k, j - 1)$ emits a spike, an increment is assigned to the corresponding synaptic conductances according to the synaptic reliability parameter, which process is given by

$$G(i, j; k, j - 1) \leftarrow G(i, j; k, j - 1) + J(i, j; k, j - 1) \cdot h(i, j; k, j - 1), \quad (2.7)$$

where $h(i, j; k, j - 1)$ denotes the synaptic reliability parameter of the synapse from neuron $(k, j - 1)$ to neuron (i, j) , and $J(i, j; k, j - 1)$ stands for the relative peak conductance of this particular excitatory synapse which is used to determine its strength. For simplicity, we assume that $J(i, j; k, j - 1) = g$, that is, the synaptic strength is identical for all excitatory connections. Parameter p is defined as the successful transmission probability of spikes. When a presynaptic neuron $(k, j - 1)$ fires a spike, we let the corresponding synaptic reliability variables $h(i, j; k, j - 1) = 1$ with probability p and $h(i, j; k, j - 1) = 0$ with probability $1 - p$. That is to say, whether the neurotransmitter is successfully released or not is in essence controlled by a Bernoulli on-off process in the present work. In other time, the synaptic conductance decays by an exponential law:

$$\frac{d}{dt}G(i, j; k, j - 1) = -\frac{1}{\tau_s}G(i, j; k, j - 1), \quad (2.8)$$

with a fixed synaptic time constant τ_s . In the case of synfire propagation, we choose $\tau_s = 2$ ms, and in the case of firing rate propagation, we choose $\tau_s = 5$ ms.

2.4 Measures of the synfire and firing rate propagation

We now introduce several useful measures used to quantitatively evaluate the performance of the two different propagation modes: the synfire mode and firing rate mode. The propagation of synfire activity is measured by the survival rate and the standard deviation of the spiking times of the synfire packet (Gewaltig et al. 2001). Let us first introduce how to calculate the survival rate for the synfire propagation. In our simulations, we find that the synfire propagation can be divided into three types: the failed synfire propagation, the stable synfire propagation, as well as the synfire instability propagation (for detail, see Sec. 3.1). For neurons in each layer, a threshold method is developed to detect the local highest ‘‘energy’’ region. To this end, we use a 5 ms moving time window with 0.1 ms sliding step to count the number of spikes within each window. Here a high energy region means that the number of spikes within the window is larger than a threshold $\theta = 50$. Since we use a moving time window with small sliding step, there might be a continuous series of windows contain more than 50 spikes around a group of synchronous spikes. In this work, we only select the first window which covers the largest number of spikes around a group of synchronous spikes as the local highest energy region. We use the number of local highest energy region to determine which type of synfire propagation occurs. If there is no local highest energy region

detected in the final layer of the network, we consider it as the failed synfire propagation. When two or more separated local highest energy regions are detected in one layer, we consider it as the synfire instability propagation. Otherwise, it means the occurrence of the stable synfire propagation. For each experimental setting, we carry out the simulation many times. The survival rate of the synfire propagation is defined as the ratio of the number of occurrence of the stable synfire propagation to the total number of simulations. In additional simulations, it turns out that the threshold value θ can vary in a wide range without altering the results. Under certain conditions, noise can help the feedforward neuronal network produce the spontaneous spike packets, which promotes the occurrence of synfire instability propagation and therefore decreases the survival rate. For stable synfire propagation, there exists only one highest energy region for neurons in each layer. Spikes within this region are considered as the candidate synfire packet, which might also contain a few spontaneous spikes caused by noise and other factors. In this work, an adaptive algorithm is introduced to eliminate spontaneous spikes from the candidate synfire packet. Suppose now that there is a candidate synfire packet in the i -th layer with the number of spikes it contains α_i and the corresponding spiking times $\{t_1, t_2, \dots, t_{\alpha_i}\}$. The average spiking time of the candidate synfire packet is therefore given by

$$\bar{t}_i = \frac{1}{\alpha_i} \sum_{k=1}^{\alpha_i} t_k. \quad (2.9)$$

Thus the standard deviation of the spiking times in the i -th layer can be calculated as follows:

$$\sigma_i = \sqrt{\frac{1}{\alpha_i} \sum_{k=1}^{\alpha_i} [t_k - \bar{t}_i]^2}. \quad (2.10)$$

We remove the j -th spike from the candidate synfire packet if it satisfies: $|t_j - \bar{t}_i| > \mu\sigma_i$, where μ is a parameter of our algorithm. We recompute the average spiking time as well as the standard deviation of the spiking times for the new candidate synfire packet, and repeat the above eliminating process, until no spike is removed from the new candidate synfire packet anymore. We define the remaining spikes as the synfire packet, which is characterized by the final values of α_i and σ_i . Parameter μ determines the performance of the proposed algorithm. If μ is too large, the synfire packet will lose several useful spikes at its borders, and if μ is too small, the synfire packet will contain some noise data. In our simulations, we found that $\mu = 4$ can result in a good compromise between these two extremes. It should be emphasized that our algorithm is inspired by the method given in (Gewaltig et al. 2001). Next, we introduce how to measure the performance of the firing rate propagation. The performance of firing rate propagation is evaluated by combining it with a population code. Specifically, we compute how similar the population firing rates in different layers to the external input current $I(t)$ (van Rossum et al. 2002; Vogels and Abbott 2005). To do this, a 5 ms moving time window with 1 ms sliding step is also used to estimate the population firing rates $r_i(t)$ for different layers as well as the smooth version of the external input current $I_s(t)$. The correlation coefficient between the population firing rate of the i -th layer and external

input current is calculated by

$$C_i(\tau) = \frac{\langle [I_s(k + \tau) - \bar{I}_s] [r_i(k) - \bar{r}_i] \rangle_t}{\sqrt{\langle [I_s(k + \tau) - \bar{I}_s]^2 \rangle_t \langle [r_i(k) - \bar{r}_i]^2 \rangle_t}}, \quad (2.11)$$

where $\langle \cdot \rangle_t$ denotes the average over time. Here we use the maximum cross-correlation coefficient $Q_i = \max\{C_i(\tau)\}$ to quantify the performance of the firing rate propagation in the i -th layer. Note that Q_i is a normalization measure and a larger value corresponds to a better performance.

2.5 Numerical simulation method

In all numerical simulations, we use the standard Euler-Maruyama integration scheme to numerically calculate the aforementioned stochastic differential Eqs. (2.1)-(2.8) (Kloeden et al. 1994). The temporal resolution of integration is fixed at 0.02 ms for calculating the measures of the synfire mode and at 0.05 ms for calculating the measures of the firing rate mode, as the measurement of the synfire needs higher precise. In additional simulations, we have found that further reducing the integration time step does not change our numerical results in a significant way. For the synfire mode, all simulations are executed at least 100 ms to ensure that the synfire packet can be successfully propagated to the final layer of the considered network. While studying the firing rate mode, we perform all simulations up to 5000 ms to collect enough spikes for statistical analysis. It should be noted that, to obtain convincing results, we carry out several times of simulations (at least 200 times for the synfire mode and 50 times for the firing rate mode) for each experimental setting to compute the corresponding measures.

3 Simulation results

In this section, we report the main results obtained in the simulation. We first systematically investigate the signal propagation in the URE feedforward neuronal networks. Then, we compare these results with those for the corresponding RRE feedforward neuronal networks. Finally, we further study the signal propagation in the UREI feedforward neuronal networks.

3.1 Synfire propagation in URE feedforward neuronal networks

Here we study the role of unreliable synapses on the propagation of synfire packet in the URE feedforward neuronal networks. In the absence of noise, we artificially let each sensory neuron fire and only fire an action potential at the same time ($\alpha_1 = 100$ and $\sigma_1 = 0$ ms). Without loss of generality, we let all sensory neurons fire spikes at $t = 10$ ms. Figure 2 shows four typical spike raster diagrams of propagating synfire activity. Note that the time scales in Figs. 2(a)-2(d) are different. The URE feedforward neuronal network with both small successful transmission probability and small

excitatory synaptic strength badly supports the synfire propagation. In this case, due to high synaptic unreliability and weak excitatory synaptic interaction between neurons, the propagation of synfire packet cannot reach the final layer of the whole network (see Fig. 2(a)). For suitable values of p and g , we find that the synfire packet can be stably transmitted in the URE feedforward neuronal network. Moreover, it is obvious that the width of the synfire packet at any layer for $p = 0.8$ is much narrower than that of the corresponding synfire packet for $p = 0.25$ (see Figs. 2(b) and 2(c)). At the same time, the transmission speed is also enhanced with the increasing of p . These results indicate that the neuronal response of the considered network is much more precise and faster for suitable large successful transmission probability. However, our simulation results also reveal that a strong excitatory synaptic strength with large value of p might destroy the propagation of synfire activity. As we see from Fig. 2(d), the initial tight synfire packet splits into several different synfire packets during the transmission process. Such phenomenon is called the “synfire instability” (Tetzlaff et al. 2002; Tetzlaff et al. 2003), which mainly results from the burst firings of several neurons caused by the strong excitatory synaptic interaction as well as the stochastic fluctuation of the synaptic connections.

In Fig. 3(a), we depict the survival rate of synfire propagation as a function of the successful transmission probability p for different values of excitatory synaptic strength g , with the noise intensity $D_t = 0$. We find that each survival rate curve can be at least characterized by one corresponding critical probability p_{on} . For small p , due to low synaptic reliability, any synfire packet cannot reach the final layer of the URE feedforward neuronal network. Once the successful transmission probability p exceeds the critical probability p_{on} , the survival rate rapidly transits from 0 to 1, suggesting that the propagation of synfire activity becomes stable for a suitable high synaptic reliability. On the other hand, besides the critical probability p_{on} , we find that the survival rate curve should be also characterized by another critical probability p_{off} if the excitatory synaptic strength is sufficiently strong (for example, $g = 3.5$ nS in Fig. 3(a)). In this case, when $p \geq p_{\text{off}}$, our simulation results show that the survival rate rapidly decays from 1 to 0, indicating that the network fails to propagate the stable synfire packet again. However, it should be noted that this does not mean that the synfire packet cannot reach the final layer of the network in this situation, but because the excitatory synapses with both high reliability and strong strength lead to the occurrence of the redundant synfire instability in transmission layers.

To systematically establish the limits for the appearance of stable synfire propagation as well as to check that whether our previous results can be generalized within a certain range of parameters, we further calculate the survival rate of synfire propagation in the (g, p) panel, which is shown in Fig. 3(b). As we see, the whole (g, p) panel can be clearly divided into three regimes. These regimes include the failed synfire propagation regime (regime I), the stable synfire propagation regime (regime II), and the synfire instability propagation regime (regime III). Our simulation results reveal that transitions between these regimes are normally very fast and therefore can be described as a sharp transition. The data shown in Fig. 3(b) further demonstrate that synfire propagation is determined by the combination of both the successful

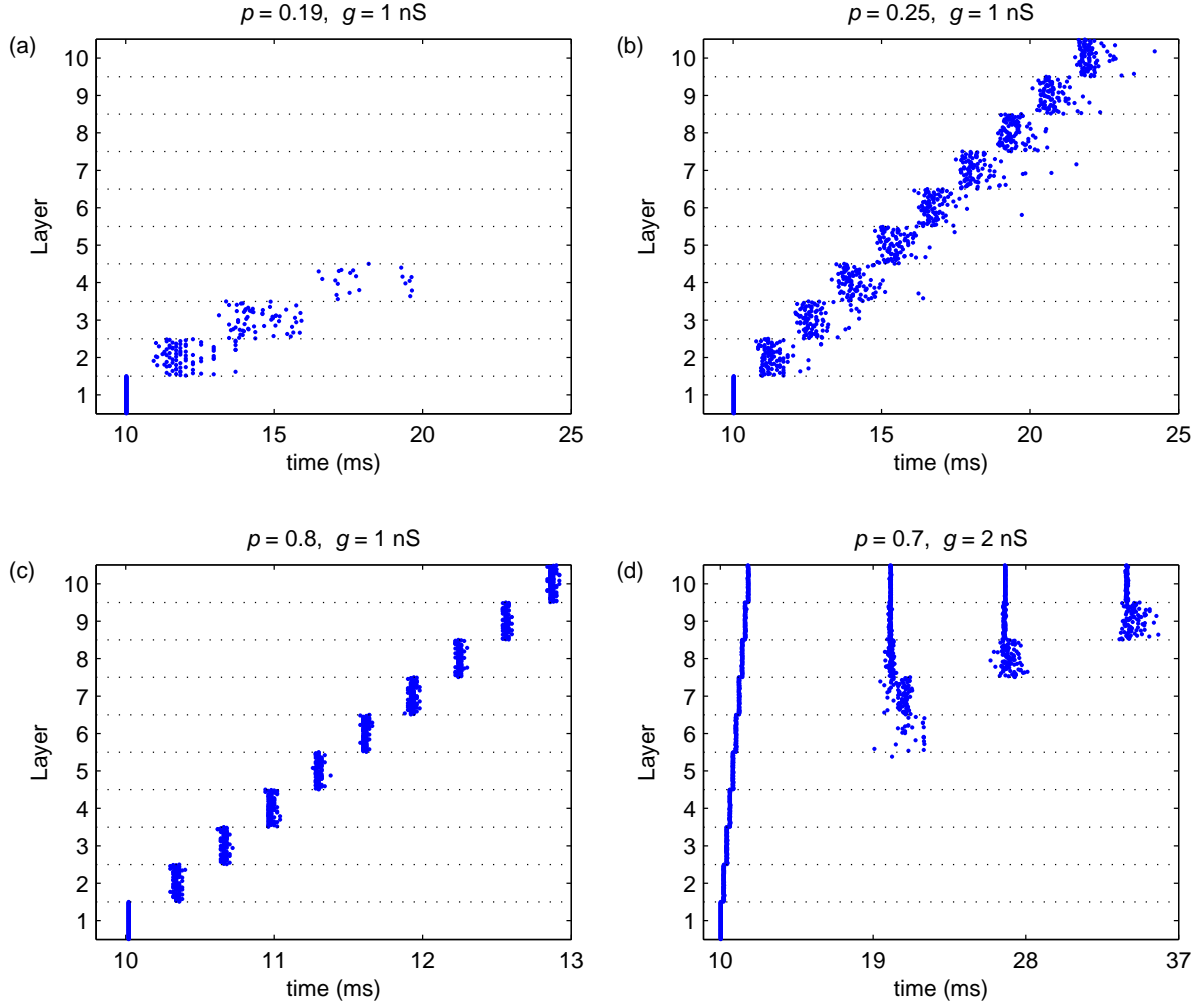


Figure 2: (Color online) Several typical spike raster diagrams for different values of successful transmission probability p and excitatory synaptic strength g . Shown are samples of (a) failed synfire propagation, (b) and (c) stable synfire propagation, and (d) synfire instability. System parameters are $p = 0.19$ and $g = 1 \text{ nS}$ (a), $p = 0.25$ and $g = 1 \text{ nS}$ (b), $p = 0.8$ and $g = 1 \text{ nS}$ (c), and $p = 0.7$ and $g = 2 \text{ nS}$ (d), respectively. As we see, the synfire packet can reach the final layer of the network successfully only for appropriate values of p and g . It should be noted that the time scales in these four subfigures are different.

transmission probability and excitatory synaptic strength. For a lower synaptic reliability, the URE feedforward neuronal network might need a larger g to support the stable propagation of synfire packet.

In reality, not only the survival rate of the synfire propagation but also its performance is largely influenced by the successful transmission probability and the strength of the excitatory synapses. In Figs. 3(c) and 3(d), we present the standard deviation of the spiking times of the output synfire packet σ_{10} for different values of p and g , respectively. Note that here we only consider parameters p and g within the stable synfire propagation regime. The results illustrated in

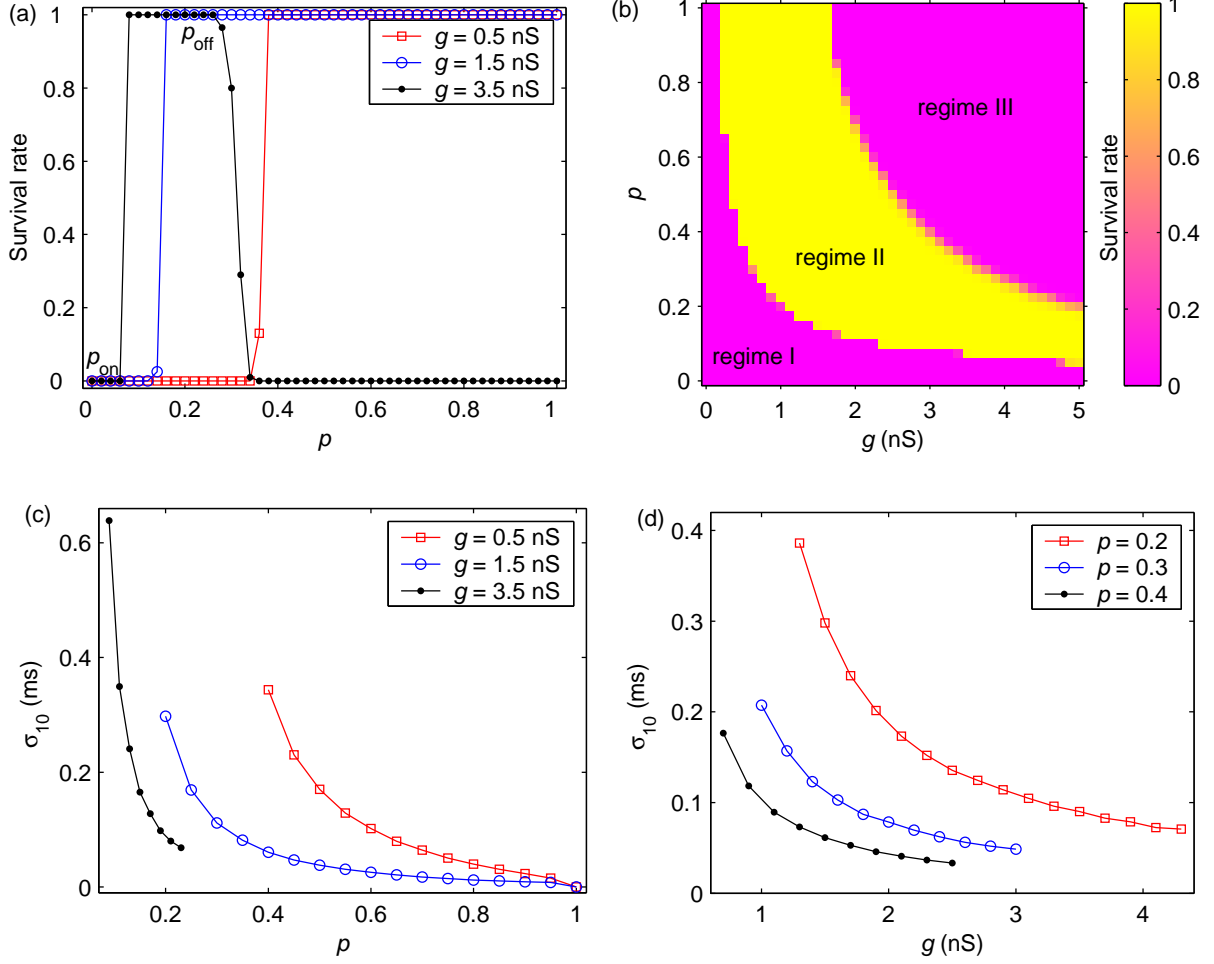


Figure 3: (Color online) Effects of the successful transmission probability and excitatory synaptic strength on the synfire propagation in URE feedforward neuronal networks. (a) The survival rate of the synfire propagation versus p for different values of g . (b) Schematic of three different synfire propagation regimes in the (g, p) panel ($41 \times 41 = 1681$ points). Regime I: the failed synfire propagation region; regime II: the stable synfire propagation region; and regime III: the synfire instability propagation region. (c) The value of σ_{10} as a function of p for different values of g . (d) The value of σ_{10} as a function of g for different values of p . In all cases, the noise intensity $D_t = 0$. Each data point shown here is computed based on 200 independent simulations with different random seeds.

Fig. 3(c) clearly demonstrate that the propagation of synfire packet shows a better performance for a suitable higher synaptic reliability. For the ideal case $p = 1$, the URE feedforward neuronal network even has the capability to propagate the perfect synfire packet ($\alpha_i = 100$ and $\sigma_i = 0$ ms) in the absence of noise. On the other hand, it is also found that for a fixed p the performance of synfire propagation becomes better and better as the value of g is increased (see Fig. 3(d)). The above results indicate that both high synaptic reliability and strong excitatory synaptic strength are able to help the URE feedforward neuronal network maintain the precision of neuronal response in the stable synfire propagation regime.

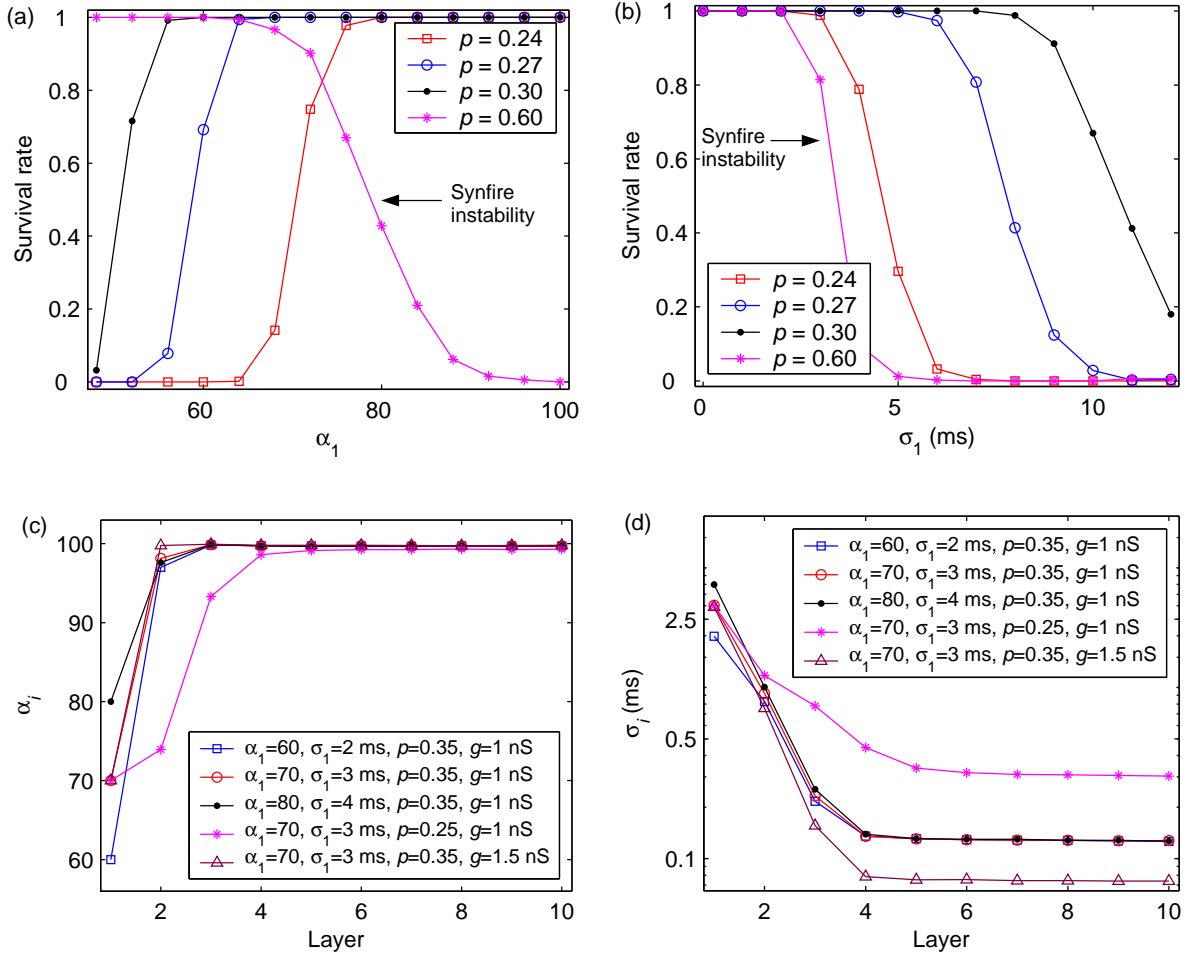


Figure 4: (Color online) Dependence of the synfire propagation on the parameters of the initial spike packet. Here we display the survival rate of the synfire propagation versus α_1 (a) and σ_1 (b) for different successful transmission probabilities, and the values of n_i (c) and σ_i (d) as a function of the layer number for different initial spike packets and different intrinsic parameters of the network, respectively. Note that the vertical axis in (d) is a log scale. In all cases, the noise intensity $D_t = 0$. Other parameters are $g = 1$ nS and $\sigma_1 = 3$ ms (a), $g = 1$ nS and $\alpha_1 = 70$ (b). Each data shown in (a) and (b) is computed based on 600 independent simulations, whereas each data shown in (c) and (d) is calculated based on 500 independent successful synfire propagation simulations.

Up to now, we only use the perfect initial spike packet ($\alpha_1 = 100$ and $\sigma_1 = 0$ ms) to evoke the synfire propagation. This is a special case which is simplified for analysis, but it is not necessary to restrict this condition. To understand how a generalized spike packet is propagated through the URE feedforward neuronal network, we randomly choose α_1 neurons from the sensory layer, and let each of these neurons fire and only fire a spike at any moment according to a Gaussian distribution with the standard deviation σ_1 . In Figs. 4(a) and 4(b), we plot the survival rate of the synfire propagation as a function of α_1 and σ_1 for four different values of successful transmission probability, respectively. When

the successful transmission probability is not too large (for example, $p = 0.24, 0.27,$ and 0.3 in Figs. 4(a) and 4(b)), the synfire activity is well build up after several initial layers for sufficiently strong initial spike packet (large α_1 and small σ_1), and then this activity can be successfully transmitted along the entire network with high survival rate. In this case, too weak initial spike packet (small α_1 and large σ_1) leads to the propagation of the neural activities becoming weaker and weaker with the increasing of layer number. Finally, the neural activities are stopped before they reach the final layer of the network. Moreover, with the increasing of the successful transmission probability, neurons in the downstream layers will share more common synaptic currents from neurons in the corresponding upstream layers. This means that neurons in the considered network have the tendency to fire more synchronously for suitable larger p (not too large). On the other hand, for sufficiently high synaptic reliability (for instance, $p = 0.6$ in Figs. 4(a) and 4(b)), a large α_1 or a suitable large σ_1 may result in the occurrence of synfire instability, which also reduces the survival rate of the synfire propagation. Therefore, for a fixed g , the URE feedforward neuronal network with suitable higher synaptic reliability has the ability to build up stable synfire propagation from a slightly weaker initial spike packet (see Figs. 4(a) and 4(b)).

Figures 4(c) and 4(d) illustrate the values of α_i and σ_i versus the layer number for different initial spike packets and several different intrinsic system parameters of the network (the successful transmission probability p and excitatory synaptic strength g). For each case shown in Figs. 4(c) and 4(d), once the synfire propagation is successfully established, n_i converges fast to the saturated value 100 and σ_i approaches to an asymptotic value. Although the initial spike packet indeed determines whether the synfire propagation can be established or not as well as influences the performance of synfire propagation in the first several layers, but it does not determine the value of σ_i in deep layers provided that the synfire propagation is successfully evoked. For the same intrinsic system parameters, if we use different initial spike packets to evoke the synfire propagation, the value of σ_i in deep layers is almost the same for different initial spike packets (see Fig. 4(d)). The above results indicate that the performance of synfire propagation in deep layers of the URE feedforward neuronal network is quite stubborn, which is mainly determined by the intrinsic parameters of the network but not the parameters of the initial spike packet. In fact, many studies have revealed that the synfire activity is governed by a stable attractor in the (α, σ) space (Diesmann et al. 1999; Diesmann et al. 2001; Diesmann 2002; Gewaltig et al. 2001). Our above finding is a signature that the stable attractor of synfire propagation does also exist for the feedforward neuronal networks with unreliable synapses.

Next, we study the dependence of synfire propagation on neuronal noise. It is found that both the survival rate of synfire propagation and its performance are largely influenced by the noise intensity. There is no significant qualitative difference between the corresponding survival rate curves in low synaptic reliable regime. However, we find important differences between these curves for small g in high synaptic reliable regime, as well as for large g in intermediate synaptic reliable regime, that is, during the transition from the successful synfire regime to the synfire instability propagation

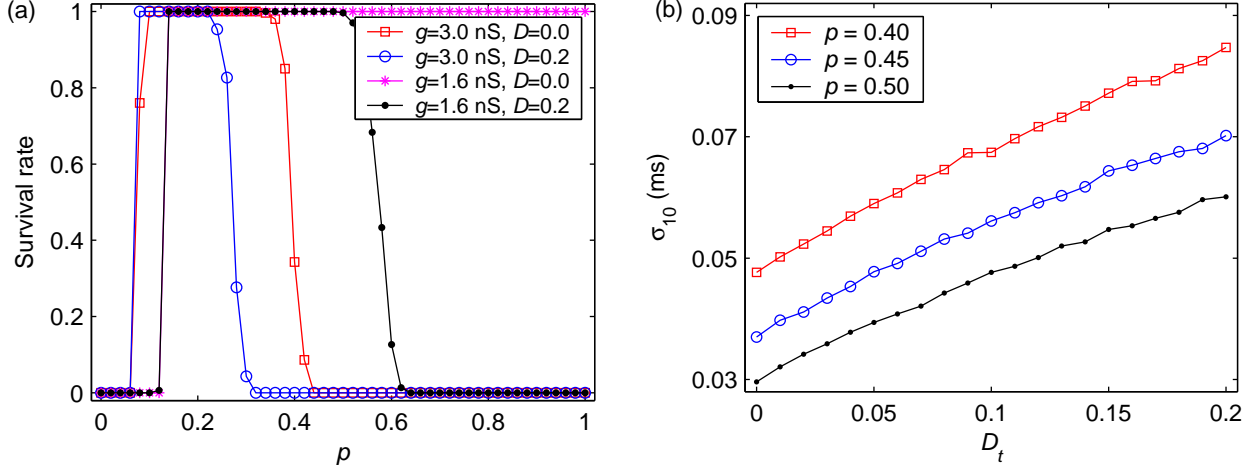


Figure 5: (Color online) Effects of the noise intensity D on the synfire propagation. (a) The survival rate versus successful transmission probability p for different excitatory coupling strength and noise intensities. (b) The value of σ_{10} versus the noise intensity D for different successful transmission probabilities, with the excitatory synaptic strength $g = 1.5$ nS. In all cases, the parameters of the initial spike packet are $\alpha_1 = 100$ and $\sigma_1 = 0$ ms. Each data shown here is computed based on 200 independent simulations with different random seeds.

regime (see from Fig. 5(a)). For each case, it is obvious that the top region of the survival rate becomes smaller with the increasing of noise intensity. This is at least due to the following two reasons: (i) noise makes neurons desynchronize, thus leading to a more dispersed synfire packet in each layer. For relatively high synaptic reliability, a dispersed synfire packet has the tendency to increase the occurrence rate of the synfire instability. (ii) Noise with large enough intensity results in several spontaneous neural firing activities at random moments, which also promote the occurrence of the synfire instability. Figure 5(b) presents the value of σ_{10} as a function of the noise intensity D_t for different values of successful transmission probability p . As we see, the value of σ_{10} becomes larger and larger as the noise intensity is increased from 0 to 0.1 (weak noise regime). This is also due to the fact that the existence of noise makes neurons desynchronize in each layer. However, although noise tends to reduce the synchrony of synfire packet, the variability of σ_i in deep layers is quite low (data not shown). The results suggest that, in weak noise regime, the synfire packet can be stably transmitted through the feedforward neuronal network with small fluctuation in deep layers, but displays slightly worse performance compared to the case of $D_t = 0$. Further increase of noise will cause many spontaneous neural firing activities which might significantly deteriorate the performance of synfire propagation. However, it should be emphasized that, although the temporal spread of synfire packet tends to increase as the noise intensity grows, several studies have suggested that under certain conditions the basin of attraction of synfire activity reaches a maximum extent (Diesmann 2002; Postma et al. 1996; Boven and Aertsen 1990). Such positive effect of noise can be compared to a well known phenomenon called

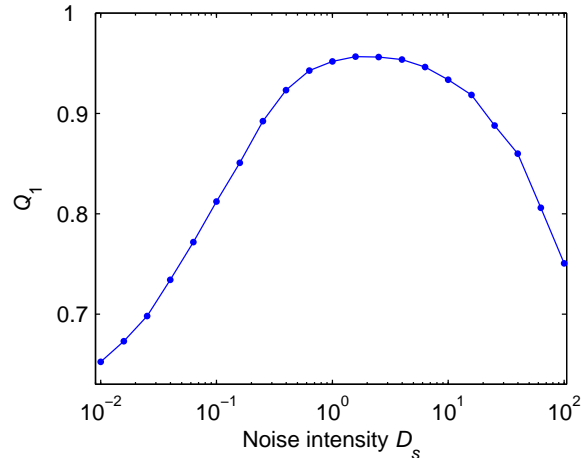


Figure 6: The maximum cross-correlation coefficient between the smooth version of external input current $I_s(t)$ and the population firing rate of sensory neurons $r_1(t)$ for different noise intensities.

aperiodic stochastic resonance (Collins et al. 1995b; Collins et al. 1996; Diesmann 2002).

3.2 Firing rate propagation in URE feedforward neuronal networks

In this subsection, we examine the firing rate propagation in URE feedforward neuronal networks. To this end, we assume that all sensory neurons are injected to a same time-varying external current $I(t)$ (see Sec. 2.2 for detail). Note now that the sensory neurons are modeled by using the integrate-and-fire neuron model in the study of the firing rate propagation.

Before we present the results of the firing rate propagation, let us first investigate how noise influences the encoding capability of sensory neurons by the population firing rate. This is an important preliminary step, because how much input information represented by sensory neurons will directly influence the performance of firing rate propagation. The corresponding results are plotted in Figs. 6 and 7, respectively. When the noise is too weak, the dynamics of sensory neurons is mainly controlled by the same external input current, which causes neurons to fire spikes almost at the same time (see Figs. 7(a) and 7(b)). In this case, the information of the external input current is poorly encoded by the population firing rate since the synchronous neurons have the tendency to redundantly encode the same aspect of the external input signal. When the noise intensity falls within a special intermediate range (about 0.5-10), neuronal firing is driven by both the external input current and noise. With the help of noise, the firing rate is able to reflect the temporal structural information (i.e., temporal waveform) of the external input current to a certain degree (see Figs. 7(c) to 7(f)), and therefore Q_1 has large value in this situation. For too large noise intensity, the external input current is almost drowned in noise, thus resulting that the input information cannot be well read from the population firing rate of sensory neurons again. On the other hand, sensory neurons can fire “false” spikes provided that they are driven by sufficiently

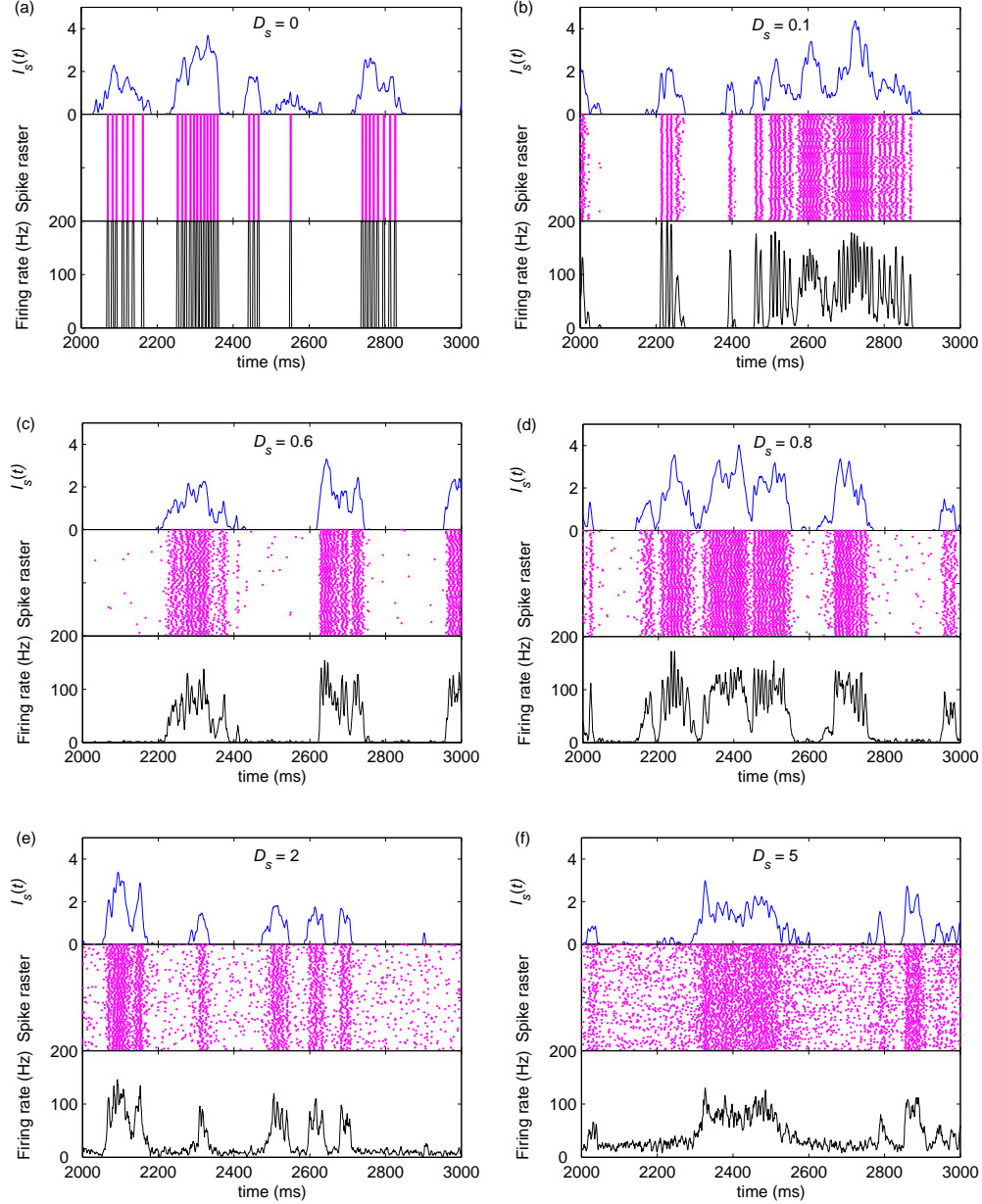


Figure 7: (Color online) Impacts of noise on the encoding performance (the firing rate mode) of sensory neurons. For each case, the smooth version of the external input current $I_s(t)$ (top panel), spike raster diagram of sensory neurons (middle panel), and population firing rate of sensory neurons (bottom panel) are shown. Noise intensities are $D_s = 0$ (a), $D_s = 0.1$ (b), $D_s = 0.6$ (c), $D_s = 0.8$ (d), $D_s = 2$ (e), and $D_s = 5$ (f), respectively.

strong noise (as for example at $t \approx 2800$ ms in Fig. 7(e)). Although the encoding performance of the sensory neurons might be good enough in this case, our numerical simulations reveal that such false spikes will seriously reduce the performance of the firing rate propagation in deep layers, which will be discussed in detail in the later part of this section. By taking these factors into account, we consider the noise intensity of sensory neurons to be within the range of 0.5 to 1 in the

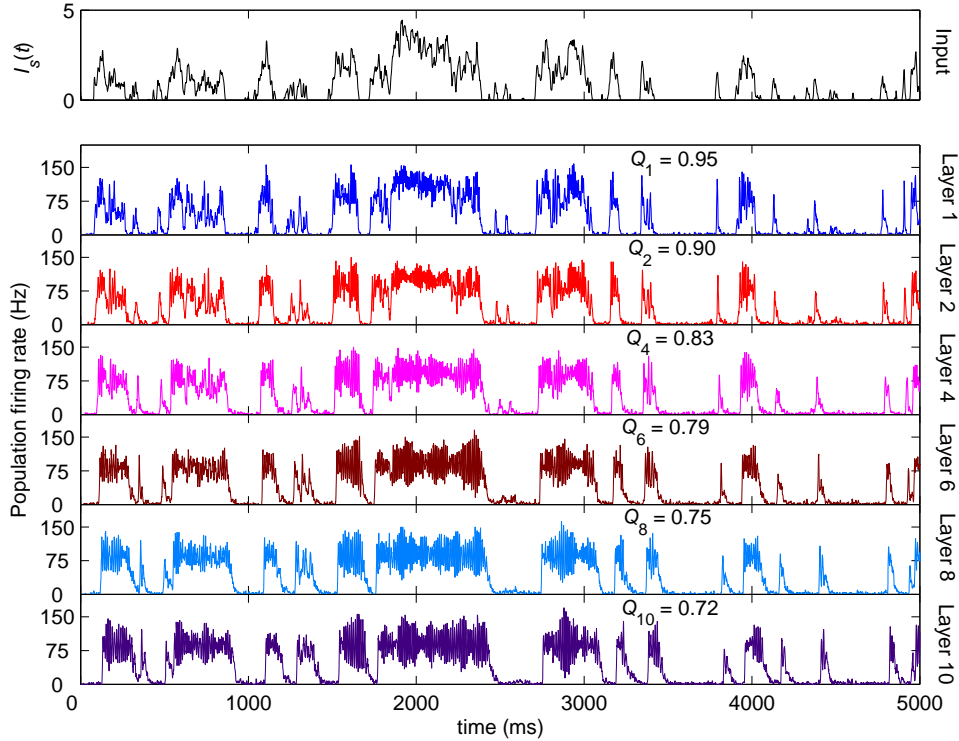


Figure 8: An example of the firing rate propagation in the URE feedforward network. Here we show the smooth version of the external input current $I_s(t)$, as and the population firing rates of layers 1, 2, 4, 6, 8, and 10, respectively. System parameters are $g = 0.4$ nS, $p = 0.2$, and $D_s = D_t = 0.7$.

present work.

Figure 8 shows a typical example of the firing rate propagation. In view of the overall situation, the firing rate can be propagated rapidly and basically linearly in the URE feedforward neuronal network. However, it should be noted that, although the firing rates of neurons from the downstream layers tend to track those from the upstream layers, there are still several differences between the firing rates for neurons in two adjacent layers. For example, it is obvious that some low firing rates may disappear or be slightly amplified in the first several layers, as well as some high firing rates are weakened to a certain degree during the whole transmission process. Therefore, as the neural activities are propagated across the network, the firing rate has the tendency to lose a part of local detailed neural information but can maintain a certain amount of global neural information. As a result, the maximum cross-correlation coefficient between $I_s(t)$ and $r_i(t)$ basically drops with the increasing of the layer number.

Let us now assess the impacts of the unreliable synapses on the performance of firing rate propagation in the URE feedforward neuronal network. Figure 9(a) presents the value of Q_{10} versus the success transmission probability p for various excitatory synaptic strengths. For a fixed value of g , a bell-shaped Q_{10} curve is clearly seen by changing the value of successful transmission probability, indicating that the firing rate propagation shows the best performance at an

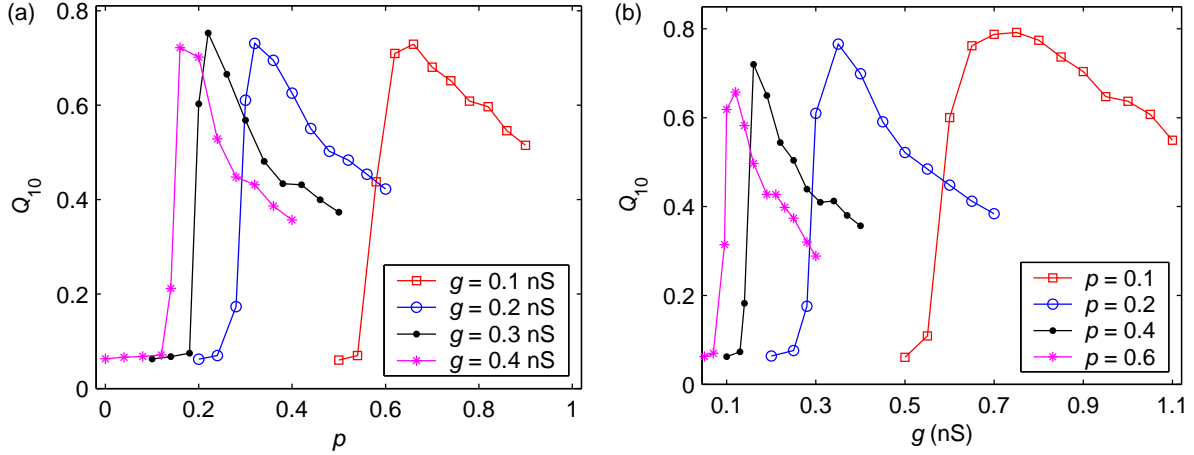


Figure 9: (Color online) Effects of the unreliable synapses on the performance of firing rate propagation. (a) The value of Q_{10} as a function of p for different values of excitatory synaptic strength. (b) The value of Q_{10} as a function of g for different values of successful transmission probability. Noise intensities are $D_s = D_t = 0.5$ in all cases. Here each data point is computed based on 50 different independent simulations with different random seeds.

optimal synaptic reliability level. This is because, for each value of g , a very small p will result in the insufficient firing rate propagation due to low synaptic reliability, whereas a sufficiently large p can lead to the excessive propagation of firing rate caused by burst firings. Based on above reasons, the firing rate can be well transmitted to the final layer of the URE feedforward neuronal network only for suitable intermediate successful transmission probabilities. Moreover, with the increasing of g , the considered network needs a relatively small p to support the optimal firing rate propagation. In Fig. 9(b), we plot the value of Q_{10} as a function of the excitatory synaptic strength g for different values of p . Here the similar results as those shown in Fig. 9(a) can be observed. This is due to the fact that increasing g and fixing the value of p is equivalent to increasing p and fixing the value of g to a certain degree. According to the aforementioned results, we conclude that both the successful transmission probability and excitatory synaptic strength are critical for firing rate propagation in URE feedforward networks, and better choosing of these two unreliable synaptic parameters can help the cortical neurons encode neural information more accurately.

Next, we examine the dependence of the firing rate propagation on neuronal noise. The corresponding results are plotted in Figs. 10 and 11, respectively. Figure 10(a) demonstrates that the noise of cortical neurons plays an important role in firing rate propagation. Noise of cortical neurons with appropriate intensity is able to enhance their encoding accuracy. It is because appropriate intermediate noise, on the one hand, prohibits synchronous firings of cortical neurons in deep layers, and on the other hand, ensures that the useful neural information does not drown in noise. However, the level of enhancement is largely influenced by the noise intensity of sensory neurons. As we see, for a large value of

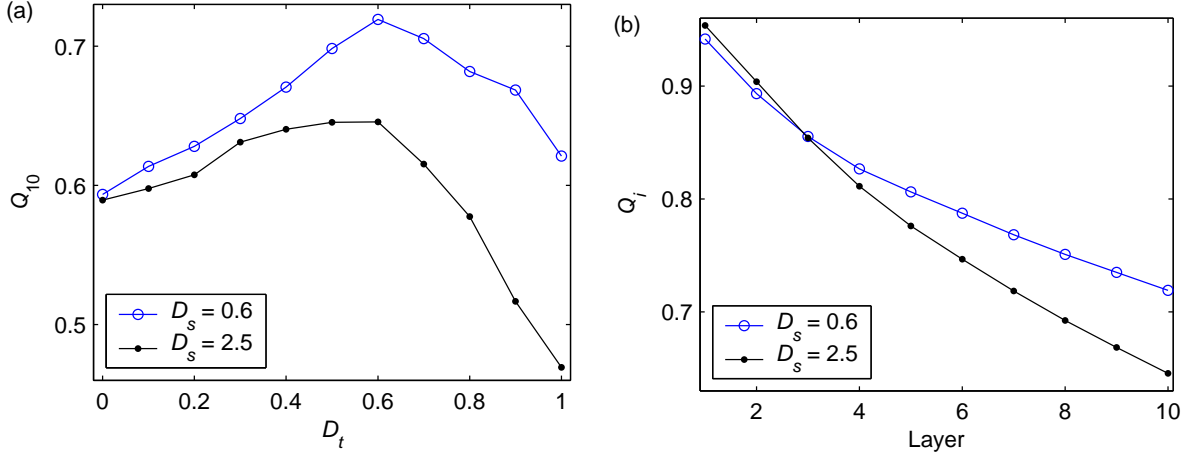


Figure 10: (Color online) Impacts of noise on the performance of firing rate propagation. (a) The value of Q_{10} as a function of the noise intensity of cortical neurons D_t for different values of D_s . (b) The performance of firing rate propagation in each layer at $D_t = 0.6$ for two different noise intensities of sensory neurons. In all cases, $p = 0.2$ and $g = 0.4$ nS. Here each data point is computed based on 50 different independent simulations with different random seeds.

D_s , such enhancement is weakened to a great extent. This is because slightly strong noise intensity of sensory neurons will cause these neurons to fire several false spikes and a part of these spikes can be propagated to the transmission layers. If enough false spikes appear around the weak components of the external input current, these spikes will help the network abnormally amplify these weak components during the whole transmission process. The aforementioned process can be seen clearly from an example shown in Fig. 11. As a result, the performance of the firing rate propagation might be seriously deteriorated in deep layers. However, it should be noted that this kind of influence typically needs the accumulation of several layers. Our simulation results show that the performance of firing rate propagation can be well maintained or even becomes slightly better (depending on the noise intensity of sensory neurons, see Fig. 6) in the first several layers for large D_s (see Fig. 10(b)). In fact, the above results are based on the assumption that each cortical neuron is driven by independent noise current with the same intensity. Our results can be generalized from the sensory layer to the transmission layers if we suppose that noise intensities for neurons in different transmission layers are different. All these results imply that better tuning of the noise intensities of both the sensory and cortical neurons can enhance the performance of firing rate propagation in the URE feedforward neuronal network.

3.3 Stochastic effect of neurotransmitter release

From the numerical results depicted in Secs. 3.1 and 3.2, we find that increasing g with p fixed has similar effects as increasing p while keeping g fixed for both the synfire mode and firing rate mode. Some persons might therefore postulate that the signal propagation dynamics in feedforward neuronal networks with unreliable synapses can be simply determined

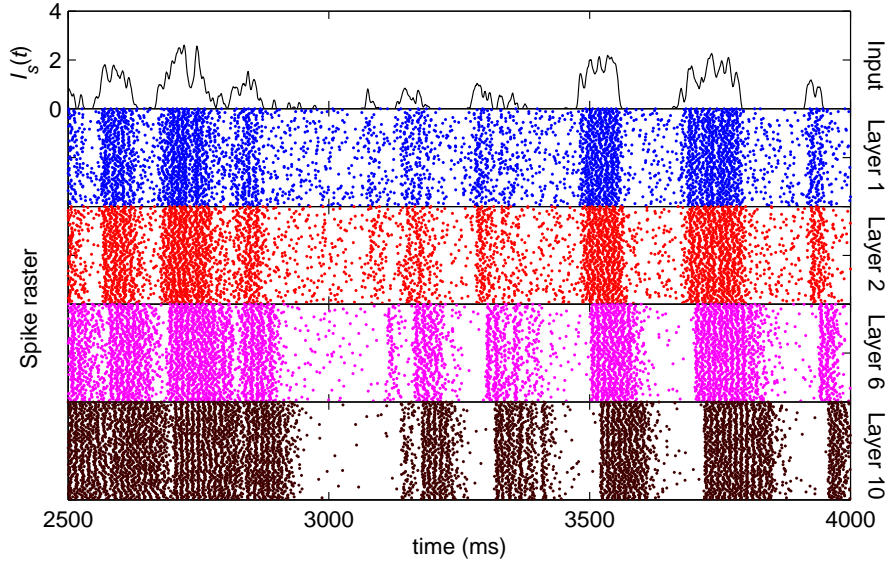


Figure 11: (Color online) An example of weak external input signal amplification. System parameters are the successful transmission probability $p = 0.2$, excitatory synaptic strength $g = 0.4$ nS, and noise intensities $D_s = 2.5$ and $D_t = 0.6$, respectively.

by the average amount of received neurotransmitter for each neuron in a time instant, which can be reflected by the product of $g \cdot p$. To check whether this is true, we calculate the measures of these two signal propagation modes as a function of $g \cdot p$ for different successful transmission probabilities. If this postulate is true, the URE feedforward neuronal network will show the same propagation performance for different values of p at a fixed $g \cdot p$. Our results shown in Figs. 12(a)-12(c) clearly demonstrate that the signal propagation dynamics in the considered network can not be simply determined by the product $g \cdot p$ or, equivalently, by the average amount of received neurotransmitter for each neuron in a time instant. For both the synfire propagation and firing rate propagation, although the propagation performance exhibits the similar trend with the increasing of $g \cdot p$, the corresponding measure curves do not superpose in most parameter region for each case, and in some parameter region the differences are somewhat significant (see Figs. 12(b) and 12(c)). This is because of the stochastic effect of neurotransmitter release, that is, the unreliability of neurotransmitter release will add randomness to the system. Different successful transmission probabilities may introduce different levels of randomness, which will further affect the nonlinear spiking dynamics of neurons. Therefore, the URE feedforward neuronal network might display different propagation performance for different values of p even at a fixed $g \cdot p$. If we set the value of $g \cdot p$ constant, a low synaptic reliability will introduce large fluctuations in the synaptic inputs. For small p , according to the above reason, some neurons will fire spikes more than once in the large $g \cdot p$ regime. This mechanism increases the occurrence rate of the synfire instability. Thus, the URE feedforward neuronal network has the tendency to stop the stable synfire propagation for a small synaptic transmission probability (see Fig. 12(a)). On the other hand, a high synaptic reliability will introduce

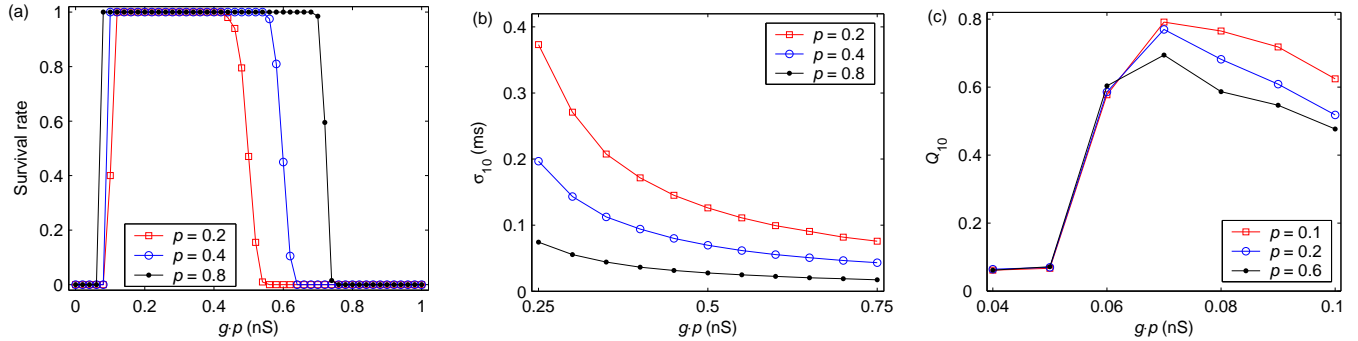


Figure 12: (Color online) Dependence of signal propagation dynamics on the product of $g \cdot p$ in the URE feedforward neuronal network. *Synfire* mode: survival rate (a) and σ_{10} versus $g \cdot p$ with $D_t = 0$. The parameters of the initial spike packet are $\alpha_1 = 100$ and $\sigma_1 = 0$ ms. *Firing rate* mode: Q_{10} as a function of $g \cdot p$ with $D_s = D_t = 0.5$. Here each data point shown in (a) and (b) is calculated based on 200 different independent simulations, whereas each data point shown in (c) are based on 50 different independent simulations.

small fluctuations in the synaptic inputs for a fixed $g \cdot p$. This makes neurons in the considered network fire spikes almost synchronously for a large p , thus resulting the worse performance for the firing rate propagation in large $g \cdot p$ regime (see Fig. 12(c)). Our above results suggest that the performance of the signal propagation in feedforward neuronal networks with unreliable synapses is not only purely determined by the change of synaptic parameters, but also largely influenced by the stochastic effect of neurotransmitter release.

3.4 Comparison with corresponding RRE feedforward neuronal networks

In this subsection, we make comparisons on the propagation dynamics between the URE and the RRE feedforward networks. We first introduce how to generate a corresponding RRE feedforward neuronal network for a given URE feedforward neuronal network. Suppose now that there is a URE feedforward neuronal network with successful transmission probability p . A corresponding RRE feedforward neuronal network is constructed by using the connection density p (on the whole), that is, a synapse from one neuron in the upstream layer to one neuron in the corresponding downstream layer exists with probability p . As in the URE feedforward neuronal network given in Sec. 2.1, there is no feedback connection from downstream neurons to upstream neurons and also no connection among neurons within the same layer in the RRE feedforward neuronal network. It is obvious that parameter p has different meanings in these two different feedforward neuronal network models. The synaptic interactions between neurons in the RRE feedforward neuronal network are also implemented by using the conductance-based model (see Eqs. (2.6) and (2.7) for detail). However, here we remove the constraint of the synaptic reliability parameter for the RRE feedforward neuronal network, e.g., $h(i, j; k, j - 1) = 1$ in

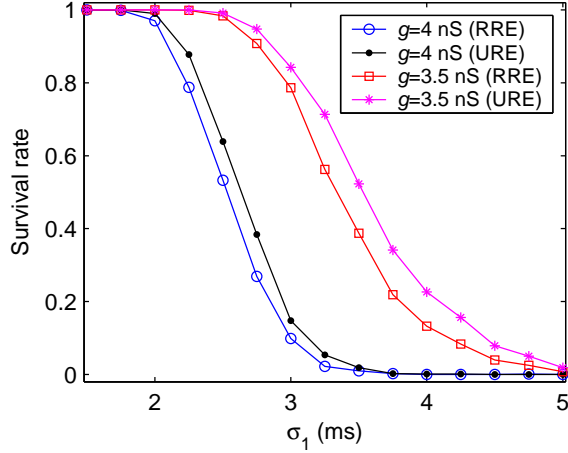


Figure 13: (Color online) The difference between the synfire propagation in the URE feedforward neuronal network and the RRE feedforward neuronal network. Here we show the value of survival rate as a function of σ_1 for different network models. In all cases, $D_t = 0$ and $\alpha_1 = 70$. Other system parameters are $g = 4$ nS and $p = 0.15$ (dot: “•”, and circle: “o”), and $g = 3.5$ nS and $p = 0.12$ (square: “□”, and asterisk: “*”). Each data point is calculated based on 500 different independent simulations with different random seeds.

all cases. A naturally arising question is what are the differences, if have, between the synfire propagation and firing propagation in URE feedforward neuronal networks and those in RRE feedforward neuronal networks, although the numbers of active synaptic connections that taking part in transmitting spikes in a time instant are the same from the viewpoint of mathematical expectation.

For the synfire propagation, our simulation results indicate that, compared to the RRE feedforward neuronal network, the URE feedforward neuronal network is able to suppress the occurrence of synfire instability to a certain degree, which can be seen clearly in Fig. 13. Typically, this phenomenon can be observed in strong excitatory synaptic strength regime. Due to the heterogeneity of connectivity, some neurons in the RRE feedforward neuronal network will have more input synaptic connections than the other neurons in the same network. For large value of g , these neurons tend to fire spikes very rapidly after they received synaptic currents. If the width of the initial spike packet is large enough, these neurons might fire spikes again after their refractory periods, which are induced by a few spikes from the posterior part of the dispersed initial spike packet. These spikes may increase the occurrence rate of the synfire instability. While in the case of URE feedforward neuronal network, the averaging effect of unreliable synapses tends to prohibit neurons fire spikes too quickly. Therefore, under the equivalent parameter conditions, less neurons can fire two or more spikes in the URE feedforeard neuronal network. As a result, the survival rate of the synfire propagation for the URE feedforeard neuronal network is larger than that for the RRE feedforward neuronal network (see Fig. 13), though not so significant.

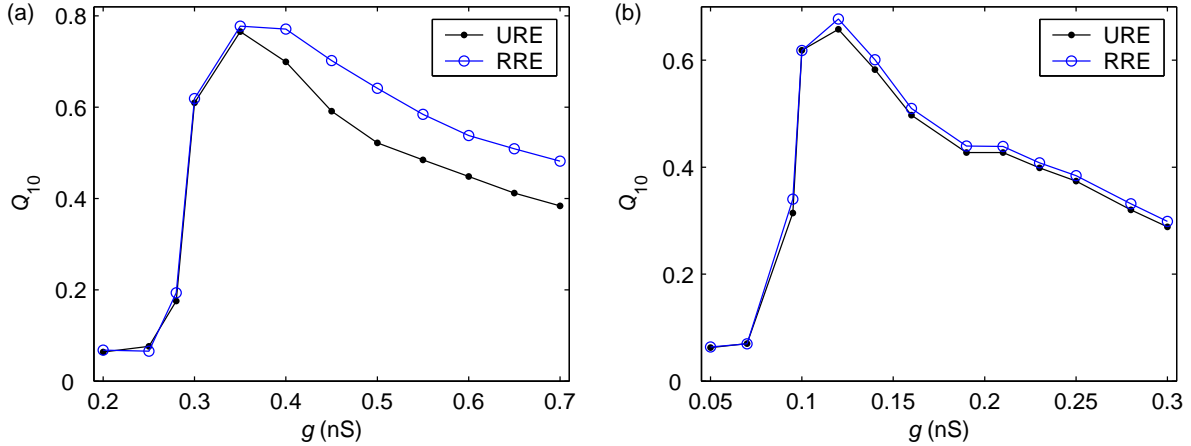


Figure 14: (Color online) Firing rate propagation in URE feedforward neuronal network and RRE feedforward neuronal network. The value of Q_{10} as a function of excitatory synaptic strength g for $p = 0.2$ (a) and $p = 0.6$ (b), respectively. Noise intensities are $D_t = D_s = 0.5$. Each data point is calculated based on 50 different independent simulations with different random seeds.

In further simulations, we find interesting results in small p regime for the firing rate propagation. Compared to the case of the URE feedforward neuronal network, the RRE feedforward neuronal network can better support the firing rate propagation in this small p regime for strong excitatory synaptic strength (see Fig. 14(a)). It is because the long-time averaging effect of unreliable synapses at small p tends to make neurons fire more synchronous spikes in the URE feedforward neuronal network through the homogenization process of synaptic currents. However, with the increasing of p , neurons in the downstream layers have the tendency to share more common synaptic currents from neurons in the corresponding upstream layers for both types of feedforward neuronal networks. The aforementioned factor makes the difference of the performance of firing rate propagation between these two types of feedforward neuronal networks become small so that the Q_{10} curves almost coincide with each other for the case of $p = 0.6$ (see Fig. 14(b)).

Although from the above results we can not conclude that unreliable synapses have advantages and play specific functional roles in signal propagation, not like those results shown in the previous studies (Goldman et al. 2002; Goldman 2004), at least it is shown that the signal propagation activities are different in URE and RRE to certain degrees. We should be cautioned when using random connections to replace unreliable synapses in modelling research. However, it should be noted that the RRE feedforward neuronal network considered here is just one type of diluted feedforward neuronal networks. There exists several other possibilities to construct the corresponding diluted feedforward neuronal networks (Hehl et al. 2001). The similar treatments for these types of diluted feedforward neuronal networks require further investigation.

3.5 Signal propagation in UREI feedforward neuronal networks

In this subsection, we further study the signal propagation in the feedforward neuronal networks composed of both excitatory and inhibitory neurons connected in an all-to-all coupling fashion (i.e., the UREI feedforward neuronal networks). This study is necessary because real biological neuronal networks, especially mammalian neocortex, consist not only of excitatory neurons but also of inhibitory neurons. The UREI feedforward neuronal network studied in this subsection has the same topology as that shown in Fig. 1. In simulations, we randomly choose 80 neurons in each layer as excitatory and the rest of them as inhibitory, as the ratio of excitatory to inhibitory neurons is about 4 : 1 in mammalian neocortex. The dynamics of the unreliable inhibitory synapse is also modeled by using Eqs. (2.6) and (2.7). The reversal potential of the inhibitory synapse is fixed at -75 mV, and its strength is set as $J = K \cdot g$, where K is a scale factor used to control the relative strength of inhibitory and excitatory synapses. Since the results of the signal propagation in UREI feedforward neuronal networks are quite similar to those in URE feedforward neuronal networks, we omit most of them and only discuss the effects of inhibition in detail.

Figure 15 shows the survival rate of synfire propagation in the (K, p) panel for three different excitatory synaptic strengths. Depending on whether the synfire packet can be successfully and stably transmitted to the final layer of the UREI feedforward neuronal network, the whole (K, p) panel can also be divided into three regimes. For each considered case, the network with both small successful transmission probability and strong relative strength of inhibitory and excitatory synapses (failed synfire regime) prohibits the stable propagation of the synfire activity. While in the case of high synaptic reliability and small K (synfire instability propagation regime), the synfire packet also cannot be stably transmitted across the whole network due to the occurrence of synfire instability. Therefore, the UREI feedforward neuronal network is able to propagate the synfire activity successfully in a stable way only for suitable combination of parameters p and K . Moreover, due to the competition between excitation and inhibition, the transitions between these different regimes cannot be described as a sharp transition anymore, in particular, for large scale factor K . Our results suggest that such non-sharp character is strengthened with the increasing of g . On the other hand, the partition of these different propagation regimes depends not only on parameters p and K but also on the excitatory synaptic strength g . As the value of g is decreased, both the synfire instability propagation regime and stable synfire propagation regime are shifted to the upper left of the (K, p) panel at first, and then disappear one by one (data not shown). In contrast, a strong excitatory synaptic strength has the tendency to extend the areas of the synfire instability propagation regime, and meanwhile makes the stable synfire propagation regime move to the lower right of the (K, p) panel.

For the case of firing rate propagation, we plot the value of Q_{10} versus the scale factor K for different excitatory synaptic strengths in Fig. 16, with a fixed successful transmission probability $p = 0.2$. When the excitatory synaptic strength is small (for instance $g = 0.4$ nS), due to weak excitatory synaptic interaction between neurons the UREI

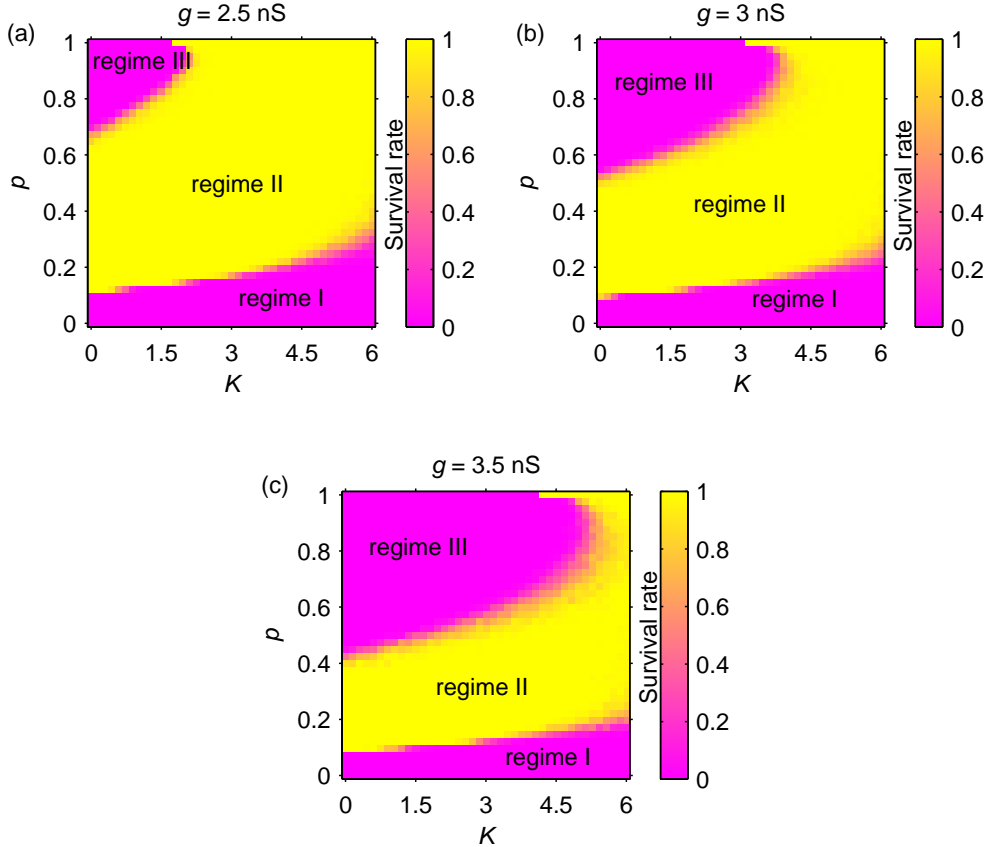


Figure 15: (Color online) Partition of three different synfire propagation regimes in the (K, p) panel ($41 \times 41 = 1681$ points). Regime I: the failed synfire propagation region; regime II: the stable synfire propagation region; and regime III: the synfire instability propagation region. we set $g = 2.5$ nS (a), $g = 3$ nS (b), and $g = 3.5$ nS (c). In all cases, the parameters of the initial spike packet are $\alpha_1 = 100$ and $\sigma_1 = 0$ ms, and the noise intensity is $D_t = 0$. Each data point shown here is calculated based on 200 different independent simulations with different random seeds.

feedforward neuronal network cannot transmit the firing rate sufficiently even for $K = 0$. In this case, less and less neural information can be propagated to the final layer of the considered network with the increasing of K . Therefore, Q_{10} monotonically decreases with the scale factor K at first and finally approaches to a low steady state value. Note that here the low steady state value is purely induced by the spontaneous neural firing activities, which are caused by the additive Gaussian white noise. As the excitatory synaptic strength grows, more neural information can be successfully transmitted for small value of K . When g is increased to a rather large value, such as $g = 0.6$ nS, the coupling is so strong that too small scale factor will lead to the excessive propagation of firing rate. However, in this case, the propagation of firing rate can still be suppressed provided that the relative strength of inhibitory and excitatory synapses is strong enough. As a result, there always exists an optimal scale factor to best support the firing rate propagation for each large excitatory

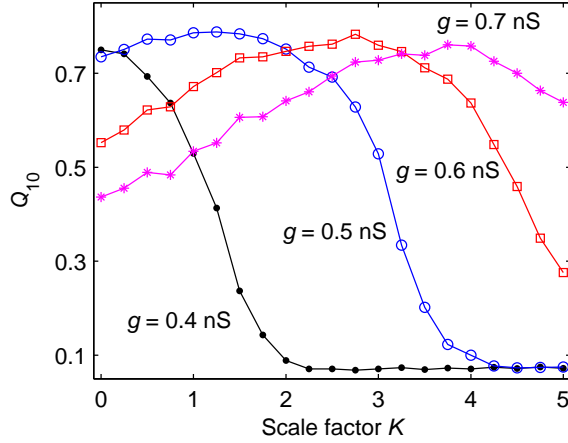


Figure 16: (Color online) Effect of inhibition on firing rate propagation. Here we show the value of Q_{10} as a function of scale factor K for different excitatory synaptic strengths. System parameters are $p = 0.2$, and $D_s = D_t = 0.6$ in all cases. Each data point is calculated based on 50 different independent simulations with different random seeds.

synaptic strength (see Fig. 16). If we fix the value of g (not too small), then the similar results can also be observed by changing the scale factor for a large successful transmission probability (data not shown). Once again, this is due to the fact that increasing g and fixing p is equivalent to increasing p and fixing g to a certain degree.

4 Conclusion and discussion

The feedforward neuronal network provides us an effective way to examine the neural activity propagation through multiple brain regions. Although biological experiments suggested that the communication between neurons is more or less unreliable (Abeles 1991; Raastad et al. 1992; Smetters and Zador 1996), so far most relevant computational studies only considered that neurons transmit spikes based on reliable synaptic models. In contrast to these previous work, we took a different approach in this work. Here we first built a 10-layer feedforward neuronal network by using purely excitatory neurons, which are connected with unreliable synapses in an all-to-all coupling fashion, that is, the so-called URE feedforward neuronal network in this paper. The goal of this work was to explore the dependence of both the synfire propagation and firing rate propagation on unreliable synapses in the URE neuronal network, but was not limited this type of feedforward neuronal network. Our modelling methodology was motivated by experimental results showing the probabilistic transmitter release of biological synapses (Branco and Staras 2009; Katz 1966; Katz 1969; Trommershäuser et al. 1999).

In the study of synfire mode, it was observed that the synfire propagation can be divided into three types (i.e., the failed synfire propagation, the stable synfire propagation, and the synfire instability propagation) depending on whether

the synfire packet can be successfully and stably transmitted to the final layer of the considered network. We found that the stable synfire propagation only occurs in the suitable region of system parameters (such as the successful transmission probability and excitatory synaptic strength). For system parameters within the stable synfire propagation regime, it was found that both high synaptic reliability and strong excitatory synaptic strength are able to support the synfire propagation in feedforward neuronal networks with better performance and faster transmission speed. Further simulation results indicated that the performance of synfire packet in deep layers is mainly influenced by the intrinsic parameters of the considered network but not the parameters of the initial spike packet, although the initial spike packet determines whether the synfire propagation can be evoked to a great degree. In fact, this is a signature that the synfire activity is governed by a stable attractor, which is in agreement with the results given in (Diesmann et al. 1999; Diesmann et al. 2001; Diesmann 2002; Gewaltig et al. 2001).

In the study of firing rate propagation, our simulation results demonstrated that both the successful transmission probability and the excitatory synaptic strength are critical for firing rate propagation. Too small successful transmission probability or too weak excitatory synaptic strength results in the insufficient firing rate propagation, whereas too large successful transmission probability or too strong excitatory synaptic strength has the tendency to lead to the excessive propagation of firing rate. Theoretically speaking, better tuning of these two synaptic parameters can help neurons encode the neural information more accurately.

On the other hand, neuronal noise is ubiquitous in the brain. There are many examples confirmed that noise is able to induce many counterintuitive phenomena, such as stochastic resonance (Collins et al. 1995a; Collins et al. 1995b; Collins et al. 1996; Chialvo et al. 1997; Guo and Li 2009) and coherence resonance (Pikovsky and Kurths 1996; Lindner and Schimansky-Geier 2002; Guo and Li 2009). Here we also investigated how the noise influences the performance of signal propagation in URE feedforward neuronal networks. The numerical simulations revealed that noise tends to reduce the performance of synfire propagation because it makes neurons desynchronized and causes some spontaneous neural firing activities. Further studies demonstrated that the survival rate of synfire propagation is also largely influenced by the noise. In contrast to the synfire propagation, our simulation results showed that noise with appropriate intensity is able to enhance the performance of firing rate propagation in URE feedforward neuronal networks. In essence, it is because suitable noise can help neurons in each layer maintain more accurate temporal structural information of the external input signal. Note that the relevant mechanisms about noise have also been discussed in several previous work (van Rossum et al. 2002; Masuda and Aihara 2002; Masuda and Aihara 2003), and our results are consistent with the findings given in these work.

Furthermore, we have also investigated the stochastic effect of neurotransmitter release on the performance of signal propagation in the URE feedforward neuronal networks. For both the synfire propagation and firing rate propagation,

we found that the URE feedforward neuronal networks might display different propagation performance, even when their average amount of received neurotransmitter for each neuron in a time instant remains unchanged. This is because the unreliability of neurotransmitter release will add randomness to the system. Different synaptic transmission probabilities will introduce different levels of stochastic effect, and thus might lead to different spiking dynamics and propagation performance. These findings revealed that the signal propagation dynamics in feedforward neuronal networks with unreliable synapses is also largely influenced by the stochastic effect of neurotransmitter release.

Finally, two supplemental work has been also performed in this paper. In the first work, we compared both the synfire propagation and firing rate propagation in URE feedforward neuronal networks with the results in corresponding feedforward neuronal networks composed of purely excitatory neurons but connected with reliable synapses in an random coupling fashion (RRE feedforward neuronal network). Our simulations showed that several different results exist for both the synfire propagation and firing rate propagation in these two different feedforward neuronal network models. These results tell us that we should be cautioned when using random connections to replace unreliable synapses in modelling research. In the second work, we extended our results to more generalized feedforward neuronal networks, which consist not only of the excitatory neurons but also of inhibitory neurons (UREI feedforward neuronal network). The simulation results demonstrated that inhibition also plays an important role in both types of neural activity propagation, and better choosing of the relative strength of inhibitory and excitatory synapses can enhance the transmission capability of the considered network.

The results presented in this work might be more realistic than those obtained based on reliable synaptic models. This is because the communication between biological neurons indeed displays the unreliable properties. In real neural systems, neurons may make full use of the characteristics of unreliable synapses to transmit neural information in an adaptive way, that is, switching between different signal propagation modes freely as required. Further work on this topic includes at least the following two aspects: (i) since all our results are derived from numerical simulations, an analytic description of the synfire propagation and firing rate propagation in our considered feedforward neuronal networks requires investigation. (ii) Intensive studies on signal propagation in the feedforward neuronal network with other types of connectivity, such as the Mexican-hat-type connectivity (Hamaguchi et al. 2004; Hamaguchi and Aihara 2005) and the Gaussian-type connectivity (van Rossum et al. 2002), as well as in the feedforward neuronal network imbedded into a recurrent network (Aviel et al. 2003; Vogels and Abbott 2005; Kumar et al. 2008), from the unreliable synapses point of view are needed as well.

Acknowledgement

We thank Feng Chen, Yuke Li, Qiuyuan Miao, Xin Wei and Qunxian Zheng for valuable discussions on an early version of this manuscript. We gratefully acknowledge the anonymous reviewers for providing useful comments and suggestion, which

greatly improved our paper. We also sincerely thank one reviewer for reminding us of a critical citation (Trommershäuser and Diesmann 2001). This work is supported by the National Natural Science Foundation of China (Grant No. 60871094), the Foundation for the Author of National Excellent Doctoral Dissertation of PR China, and the Fundamental Research Funds for the Central Universities (Grant No. 1A5000-172210126). Daqing Guo would also like to thank the award of the ongoing best PhD thesis support from the University of Electronic Science and Technology of China.

References

- [1] Abeles, M. (1991). *Corticonics: Neural circuits of the cerebral cortex*. New York: Cambridge University Press.
- [2] Aertsen, A., Diesmann, M., & Gewaltig, M. O. (1996). Propagation of synchronous spiking activity in feedforward neural networks. *J Physiology*, 90, 243-247.
- [3] Allen, C., & Stevens, C. F. (1994). An evaluation of causes for unreliability of synaptic transmission. *Proc. Natl. Acad. Sci. USA*, 91, 10380-10383.
- [4] Aviel, Y., Mehring, C., Abeles, M., & Horn, D. (2003). On embedding synfire chains in a balanced network. *Neural Computation*, 15, 1321-1340.
- [5] Boven, K., H., & Aertsen, A., M., H., J. (1990). Dynamics of activity in neuronal networks give rise to fast modulations of functional connectivity. In *Parallel processing and neural systems and computers* (pp. 53-56). Amsterdam: Elsevier.
- [6] Branco, T., & Staras, K. (2009). The probability of neurotransmitter release: variability and feedback control at single synapses. *Nature Reviews Neuroscience*, 10, 373-383.
- [7] Câteau, H., & Fukai, T. (2001). Fokker-Planck approach to the pulse packet propagation in synfire chain. *Neural Networks*, 14, 675-685.
- [8] Chialvo, D. R., Longtin, A., & Muller-Gerking, J. (1997). Stochastic resonance in models of neuronal ensembles. *Phys. Rev. E*, 55, 1798-1808.
- [9] Collins, J. J., Chow, C. C., & Imhoff, T. T. (1995a). Stochastic resonance without tuning. *Nature*, 376, 236-238.
- [10] Collins, J. J., Chow, C. C., & Imhoff, T. T. (1995b). Aperiodic stochastic resonance in excitable systems. *Phys. Rev. E* 52, R3321-R3324.
- [11] Collins, J. J., Chow, C. C., Capela, A. C., & Imhoff, T. T. (1996). Aperiodic stochastic resonance. *Phys. Rev. E*, 54, 5575-5584.

- [12] Dayan, P., & Abbott, L. F. (2001). *Theoretical neuroscience: Computational and mathematical modeling of neural systems*. Cambridge: MIT Press.
- [13] Diesmann, M., Gewaltig, M. O., & Aertsen, A. (1999). Stable propagation of synchronous spiking in cortical neural networks. *Nature*, 402, 529-533.
- [14] Diesmann, M., Gewaltig, M., O., Rotter, S., & Aertsen, A. (2001). State Space Analysis of Synchronous Spiking in Cortical Neural Networks. *Neurocomputing*, 38-40, 565-571.
- [15] Diesmann, M. (2002). Conditions for stable propagation of synchronous spiking in cortical neural networks: single neuron dynamics and network properties. PhD thesis, University of Bochum.
- [16] Friedrich, J., & Kinzel, W. (2009). Dynamics of recurrent neural networks with delayed unreliable synapses: metastable clustering. *J. Comput. Neurosci.*, 27, 65-80.
- [17] Gewaltig, M. O., Diesmann, M., & Aertsen, A. (2001). Propagation of cortical synfire activity: survival probability in single trials and stability in the mean. *Neural Networks*, 14, 657-673.
- [18] Goldman, M. S., Maldonado, P., & Abbott, L. F. (2002). Redundancy reduction and sustained firing with stochastic depressing synapses. *J. Neurosci.*, 22, 584-591.
- [19] Goldman, M. S. (2004). Enhancement of information transmission efficiency by synaptic failures. *Neural Computation*, 16, 1137-1162.
- [20] Guo, D., Q., & Li, C., G. (2009). Stochastic and coherence resonance in feed-forward-loop neuronal network motifs. *Phys. Rev. E*, 79, 051921.
- [21] Hamaguchi, K., & Aihara, K. (2005). Quantitative information transfer through layers of spiking neurons connected by Mexican-Hat-type connectivity. *Neurocomputing*, 58-60, 85-90.
- [22] Hamaguchi, K., Okada, M., Yamana, M., & Aihara, K. (2005). Correlated firing in a feedforward network with mexican-hat-type connectivity. *Neural Computation*, 17, 2034-2059.
- [23] Hehl, U., Hellwig, B., Rotter, S., Diesmann, M., Aertsen, A. (2001). Localization of synchronous spiking as a result of anatomical connectivity. *Soc. of Neuroscience*, 64, 1.
- [24] Katz, B. (1966). *Nerve, muscle and synapse*. New York: McGraw-Hill.
- [25] Katz, B. (1969). *The release of neural transmitter substances*. Liverpool, Liverpool University Press.

- [26] Kloeden P. E., Platen E., & Schurz H. (1994). *Numerical solution of SDE through computer experiments*. Berlin, Springer-Verlag Press.
- [27] Kumar A., Rotter, S., & Aertsen, A., (2008). Conditions for propagating synchronous spiking and asynchronous firing rates in a cortical network model. *J. Neurosci.*, 28, 5268-5280.
- [28] Kumar A., Rotter, S., & Aertsen, A., (2010). Spiking activity propagation in neuronal networks: reconciling different perspectives on neural coding. *Nat. Revs. Neurosci.*, 11, 615-627.
- [29] Lindner, B., & Schimansky-Geier, L. (2002). Maximizing spike train coherence or incoherence in the leaky integrate-and-fire model. *Phys. Rev. E*, 66, 031916.
- [30] Maass W., & Natschläger T. (2000). A model for fast analog computation based on unreliable synapses. *Neural Computation*, 12, 1679-1704.
- [31] Masuda, N., & Aihara, K., (2002). Bridging rate coding and temporal spike coding by effect of noise. *Phys. Rev. Lett.*, 88, 248101.
- [32] Masuda, N., & Aihara, K., (2003). Duality of rate coding and temporal coding in multilayered feedforward networks. *Neural Computation*, 15, 103-125.
- [33] Nordlie, E., Gewaltig, M., O., & Plesser, H., E. (2009). Towards reproducible descriptions of neuronal network models. *PLoS Computational Biological*, 5, e1000456.
- [34] Pikovsky, A. S., & Kurths, J. (1996). Coherence resonance in a noise-driven excitable system, *Phys. Rev. Lett.*, 78, 775-778.
- [35] Postma, E., O., van den Herik, H., J., & Hudson, P., T., W. (1996). Robust feedforward processing in synfire chains. *Int. J. Neural. Sys.*, 7, 537-542.
- [36] Raastad, M., Storm, J. F., & Andersen P. (1992). Putative single quantum and single fibre excitatory postsynaptic currents show similar amplitude range and variability in rat hippocampal slices. *Eur. J. Neurosci.*, 4, 113-117.
- [37] Rosenmund, C., Clements, J. D., & Westbrook, G. L. (1993). Nonuniform probability of glutamate release at a hippocampal synapse. *Science*, 262, 754-757.
- [38] Shinozaki, T., Câteau, H., Urakubo, H., & Okada, M. (2007). Controlling synfire chain by inhibitory synaptic input. *Journal of the Physical Society of Japan*, 76, 044806.

- [39] Shinozaki, T., Okada, M., Reyes, A. D., & Câteau, H. (2010). Flexible traffic control of the synfire-mode transmission by inhibitory modulation: Nonlinear noise reduction. *Phys. Rev. E*, 81, 011913.
- [40] Smetters, D. K., & Zador, A. (1996). Synaptic transmission: Noisy synapses and noisy neurons. *Current Biology*, 6, 1217-1218.
- [41] Stevens, C. F., & Wang, Y. (1995). Facilitation and depression at single central synapses. *Neuron*, 14, 795-802.
- [42] Tetzlaff, T., Geisel, T., & Diesmann, M. (2002), The ground State of cortical feed-forward networks. *Neurocomputing* 44-46, 673-678.
- [43] Tetzlaff, T., Buschermöhle, M., Geisel, T., & Diesmann, M. (2003), The spread of rate and correlation in stationary cortical networks, *Neurocomputing*, 52-54, 949-954.
- [44] Trommershäuser J., Marienhagen J., & Zippelius A. (1999), Stochastic model of central synapses: slow diffusion of transmitter interacting with spatially distributed receptors and transporters. *J Theor. Biol.*, 198, 101-120.
- [45] Trommershäuser, J., & Diesmann, M. (2001), The effect of synaptic variability on the synchronization dynamics in feed-forward cortical networks. In *Soc. of Neuroscience*, 64, 4.
- [46] van Rossum, M. C. W., Turrigiano, G. G., & Nelson, S. B. (2002). Fast propagation of firing rates through layered networks of noisy neurons. *J. Neurosci.*, 22, 1956-1966.
- [47] Vogels, P. T., & Abbott, L. F. (2005). Signal propagation and logic gating in networks of integrate-and-fire neurons. *J. Neurosci.*, 25, 10786-10795.
- [48] Wang, S. T., Wang, W., & Liu, F. (2006). Propagation of firing rate in a feed-forward neuronal network. *Phys. Rev. Lett.*, 96, 018103, 2006.
- [49] Wang, S. T., & Zhou, C. S. (2009). Information encoding in an oscillatory network. *Phys. Rev. E*, 79, 061910, 2009.